New Didecyloxyphenylene−Acceptor Alternating Conjugated Copolymers: Synthesis, Properties, and Optoelectronic Device Applications

Cheng-Liang Liu,[†] Jung-Hsun Tsai,[†] Wen-Ya Lee,[†] Wen-Chang Chen,*[,‡] and Samson A. Jenekhe*[,§]

Department of Chemical Engineering, National Taiwan University, Taipei 106 Taiwan; Institute of Polymer Science and Engineering, National Taiwan University, Taipei 106 Taiwan; and Departments of Chemical Engineering and of Chemistry, University of Washington, Seattle, Washington 98105-1750

Received March 4, 2008; Revised Manuscript Received May 14, 2008

ABSTRACT: Seven donor−acceptor copolymers incorporating didecyloxyphenylene (**DP**) donor and the following acceptors—thieno[3,4-*b*]pyrazine (**TP**), 2,1,3-benzothiadiazole (**BT**), quinoxaline (**Q**), pyridine (**Py**), 2,3-dimethyl-5,7-dithien-2-yl-thieno[3,4-*b*]pyrazine (**DTTP**), 4,7-dithien-2-yl-2,1,3-benzothiadiazole (**DTBT**), and 2,3-dimethyl-5,7-dithien-2-yl-quinoxaline (**DTQ**)—were synthesized by Suzuki coupling polymerization. The effects of the acceptor strength and backbone planarity on the optical, electrochemical, field-effect charge transport, and photovoltaic properties of the donor−acceptor copolymers were investigated. The optical band gap (eV) of the copolymers showed the trend of **DP/TP** (1.47) < **DP/BT** (2.37) < **DP/Py** (2.76) < **DP/Q** (2.78) < **DP/P** (3.15). The **DP/TP** copolymer had a field-effect hole mobility of 1.89×10^{-3} cm^2 V^{-1} s^{-1}. The **DP/DTBT** and **DP/DTQ** copolymers showed hole mobilities of 1.92×10^{-4} and 2.10×10^{-3} cm^2 V^{-1} s^{-1}, respectively. The strong acceptor strength of **TP** and coplanar backbone in the **DP/TP** copolymer resulted in a large intramolecular charge transfer, leading to the observed charge transport and optical properties.. These results show that the backbone planarity of the **DP/BT** and **DP/Q** copolymers was significantly improved by incorporating thiophene moieties, leading to enhanced charge transport. Photovoltaic cells fabricated from **DP/DTBT** and **DP/DTQ** polymers blended with [6,6]-phenyl-C61-butyric acid methyl ester (PCBM) showed power conversion efficiencies of 0.40−0.41% under AM 1.5 solar simulator illumination (100 mW/cm^2). The results of the present study show that the electronic and optoelectronic properties of dialkoxylphenylene-based donor−acceptor copolymers could be tuned through the acceptor structure and backbone coplanarity.

Introduction

Donor−acceptor (D−A) conjugated copolymers have attracted considerable attention in part because their electronic and optoelectronic properties could be efficiently tuned by intramolecular charge transfer (ICT).[1−18] The hybridization of the HOMO on the donor moiety and the LUMO on the acceptor moiety provides a means to tune the electronic and optoelectronic properties for device applications, such as light-emitting diodes (LEDs),[1,2a,e,3] photovoltaic cells,[4−6] field-effect transistors (FETs),[2c,d,7−9] reversible electrochromic devices,[10] and memory devices.[11]

Among the D−A alternating conjugated polymers, the electron-donating moieties of fluorene,[1−3] thiophene,[4−10] ethylenedioxythiophene,[12,13] dialkoxylphenylene,[14−19] carbazole,[20a−c] and phenothiazine[20c−f] have been reported. High FET carrier mobilities were obtained from the thiophene−acceptor or thiophene−acceptor−thiophene polymer systems through the manipulation of intramolecular charge transfer, morphology, or gate dielectric surface modification.[7−9] Our study on the fluorene-based donor−acceptor−donor polymers showed that the hole mobility was controlled by the acceptor strength and backbone coplanarity.[2c] Also, photovoltaic devices with high power conversion efficiency could be achieved through the manipulation of the acceptor structure in different donor−acceptor copolymers.[4−6]

Poly(*p*-phenylene) (**PPP**)[21,22] is a blue emitter with large band gap, and its electronic optoelectronic properties could be easily modified through side chains or copolymers. Introduction of long dialkoxy chains into the phenylene not only makes these materials more soluble but also increases the p-type strength. Recently, the synthesis and characterization of dialkoxyphenylene−acceptor conjugated copolymers have been reported.[14−19] Dialkoxyphenylene−pyridine copolymers exhibited efficient blue emission,[14,19] and their photophysical properties could be controlled by protonation/intramolecular hydrogen bonding[18] and metal ion.[15] However, the effects of acceptor strengths on the electronic and optoelectronic properties of soluble dialkoxyphenylene−acceptor and donor−acceptor−donor copolymers have not been fully explored yet, especially the field-effect charge transport and photovoltaic properties.

In this paper, we report the synthesis and properties of seven didecyloxyphenylene−acceptor or thiophene−acceptor−thiophene copolymers shown in Scheme 1. These donor−acceptor conjugated polymers were synthesized by Suzuki coupling reaction of 2,5-didecyloxy-1,4-phenylene-1,4-bis(4,4,5,5-tetramethyl-1,3,2-dioxaborolate) (**DP**) with the dibromo acceptors. The acceptors include thieno[3,4-*b*]pyrazine (**TP**), 2,1,3-benzothiadiazole (**BT**), quinoxaline (**Q**), pyridine (**Py**), 2,3-dimethyl-5,7-dithien-2-yl-thieno[3,4-*b*]pyrazine (**DTTP**), 4,7-dithien-2-yl-2,1,3-benzothiadiazole (**DTBT**), and 2,3-dimethyl-5,7-dithien-2-ylquinoxaline] (**DTQ**). The properties of these D−A copolymers could be compared those of the parent didecyloxyphenylene-phenylene polymer (**DP/P**, **1** in Scheme 1). The LUMO of the **Q**, **BT**, and **TP** moieties are −0.90, −1.81, and −1.41 eV, respectively,[23] which means that the order of the acceptor strength is **BT** > **TP** > **Q**. Thus, the effects of the acceptor strength and structural coplanarity on the optical and electro-

* To whom all correspondence should be addressed. E-mail: chenwc@ntu.edu.tw; jenekhe@u.washington.edu.
[†] Department of Chemical Engineering, National Taiwan University.
[‡] Institute of Polymer Science and Engineering, National Taiwan University.
[§] University of Washington.

10.1021/ma800488g CCC: $40.75
Published on Web 08/27/2008

Scheme 1. Synthetic Scheme of Didecyloxyphenylene-Based Donor−Acceptor and Donor−Acceptor−Donor Alternating Copolymers

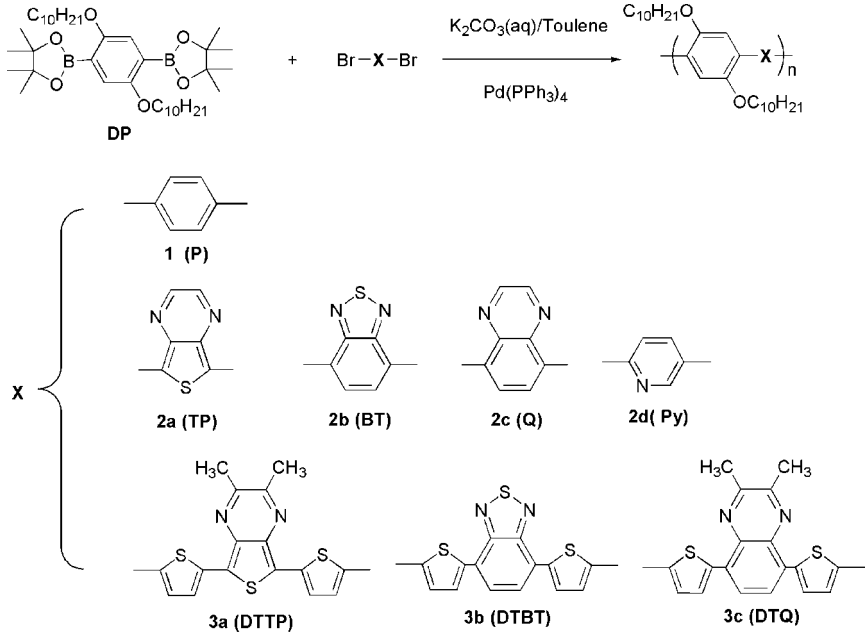

chemical properties were studied. The field-effect carrier mobility was obtained from the bottom gate thin film transistor (TFT) devices and correlated with the polymer structures. Polymer solar cell devices were fabricated by spin-coating a blend of polymer/PCBM, sandwiched between a transparent anode (ITO/**PEDOT:PSS**) and a cathode (Ca). The experimental results revealed the importance of the acceptor strength and backbone planarity on the electronic and optoelectronic properties of the didecyloxyphenylene-based donor−acceptor conjugated copolymers.

Experimental Section

Materials. 2,5-Didecyloxy-1,4-phenylene-1,4-bis(4,4,5,5-tetramethyl-1,3,2-dioxaborolate),[9] 5,7-dibromo-thieno[3,4-*b*]-pyrazine,[24] 4,7-dibromo-2,1,3-benzothiadiazole,[25] 5,8-dibromoquinoxaline,[26] 2,3-dimethyl-5,7-bis[5′-bromodithien-2-yl-thieno[3,4-*b*]-pyrazine],[2c] 2,3-dimethyl-5,8-bis[5′-bromodithien-2-yl-quinoxalines],[2c] and 4,7-di-2-thienyl-2,1,3-benzothiadiazole[2c] were synthesized similar to those reported in the literature. Tetrakis(triphenylphosphine)palladium(0), trioctylmethylammonium chloride (Aliquat 336), 2,5-dibromopyridine, 1,4-dibromopheneylene, 1,2,4-trichlorobenzene, octyltrichlorosilane (OTS, 97%), toluene, and chloroform were purchased from Aldrich or TEDIA and used without further purification. [6,6]-Phenyl-C61-butyric acid methyl ester (PCBM) was purchased from Nano-C without further purification.

General Procedures of Polymerization. Suzuki cross-coupling reaction was used to synthesize the polymers shown in Figure 1. 2,5-Didecyloxy-1,4-phenylene-1,4-bis(4,4,5,5-tetramethyl-1,3,2-dioxaborolate) (**DP**), dibromo monomer (**TP**, **BT**, **Q**, **Py**, **DTTP**, **DTBT**, **DTQ**, or **P**), and $(PPh_3)_4Pd(0)$ (1 mol % with respect to the monomer) were dissolved in a mixture of toluene (15 mL) and

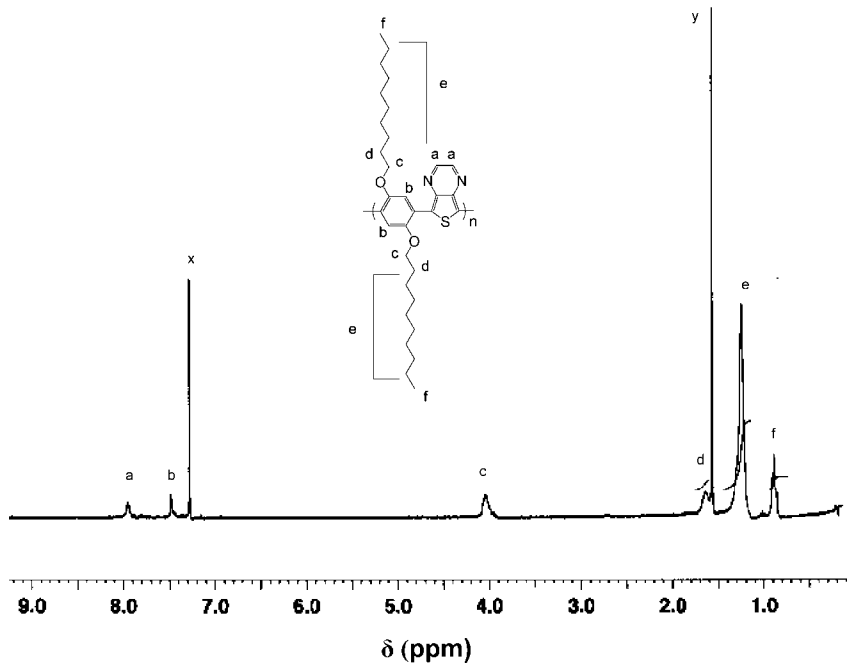

Figure 1. ^1H NMR spectrum of polymer **2a** in $CDCl_3$ solvent (x: $CDCl_3$; y: H_2O).

aqueous 2 M K_2CO_3 (3/2 volume ratio) with several drops of Aliquat 336. The solution was stirred under an Ar atmosphere and refluxed with vigorous stirring for 72 h. The resulting solution was then poured into methanol and followed by washing with water. The precipitated solid was dissolved in THF and then reprecipitated in methanol/acetone to afford the polymers. The solid product was extracted with acetone for 24 h in a Soxhlet apparatus to remove the oligomers and catalyst residues.

Poly[2,5-didecyloxy-1,4-phenylene-*alt*-1,4-phenylene)] (DP/P, 1). 350 mg of the 2,5-didecyloxy-1,4-phenylene-1,4-bis(4,4,5,5-tetramethyl-1,3,2-dioxaborolate) (**DP**) (0.54 mmol), 128 mg of 1,4-dibromopheneylene (0.54 mmol), and 15 mL of toluene were used to afford jasper solid (yield: 45%). ^{1}H NMR ($CDCl_3$, δ ppm): 7.90−7.05 (br, 6H), 3.98 (m, 4H), 1.77 (m, 4H), 1.65−1.08 (br, 28H), 0.87 (s, 6H). Anal. Calcd for $(C_{32}H_{50}O_2)_n$: C, 82.35; H, 10.80. Found: C, 80.87; H, 10.50.

Poly[2,5-didecyloxy-1,4-phenylene-*alt*-5,7-(thieno[3,4-*b*]pyrzaine)] (DP/TP, 2a). 400 mg of **DP** (0.62 mmol) and 183 mg of 5,7-dibromothieno[3,4-*b*]pyrazine (0.62 mmol) were used to afford a dark green solid (yield: 47%). ^{1}H NMR ($CDCl_3$, δ ppm): 7.95 (s, 2H), 7.47 (s, 2H), 4.05 (m, 4H), 1.65 (m, 4H), 1.23 (br, 28H), 0.89 (s, 6H). Calcd for $((C_{32}H_{48}O_2N_2S)_n$: C, 73.24; H, 9.22; N, 5.34; S, 6.11. Found: C, 72.13; H, 9.15; N, 5.19; S, 5.62.

Poly[2,5-didecyloxy-1,4-phenylene-*alt*-4,7-(2,1,3-benzothiodiazole)] (DP/BT, 2b). 500 mg of **DP** (0.78 mmol) and 229 mg of 4,7-dibromo-2,1,3-benzothiodiazole (0.78 mmol) were used to afford a yellowish-brown solid (yield: 55%). ^{1}H NMR ($CDCl_3$, δ ppm): 8.68 (br, 2H), 8.61 (br, 2H), 4.11 (m, 4H), 1.90−0.95 (br, 32H), 0.89 (s, 6H). Anal. Calcd for $(C_{32}H_{48}O_2N_2S)_n$: C, 73.24; H, 9.22; N, 5.34; S, 6.11. Found: C, 72.09; H, 9.11; N, 5.17; S, 5.65.

Poly[2,5-didecyloxy-1,4-phenylene-*alt*-(5,8-quinoxaline)] (DP/Q, 2c). 500 mg of **DP** (0.78 mmol) and 224 mg of 5,8-dibromoquinoxaline (0.78 mmol) were used to afford an olivine solid (yield: 60%). ^{1}H NMR ($CDCl_3$, δ ppm): 8.93 (s, 2H), 8.01 (s, 2H), 7.25 (s, 2H), 3.95 (m, 4H), 1.60−0.95 (br, 32H), 0.89 (s, 6H). Anal. Calcd for $(C_{34}H_{50}O_2N_2)_n$: C, 78.72; H, 9.71; N, 5.40. Found: C, 77.83; H, 9.65; N, 5.31.

Poly[2,5-didecyloxy-1,4-phenylene-*alt*-(2,5-pyridine)] (DP/Py, 2d). 500 mg of **DP** (0.78 mmol) and 184 mg of 2,5-dibromopyridine (0.78 mmol) were used to afford an olivine solid (yield: 80%). ^{1}H NMR ($CDCl_3$, δ ppm): 8.97 (s, 1H), 8.17 (br, 1H), 8.03 (br, 1H), 7.75 (br, 1H), 7.10 (br, 1H), 4.11 (m, 4H), 1.90−0.95 (br, 32H), 0.89 (s, 6H). Anal. Calcd for $(C_{31}H_{49}O_2N)_n$: C, 79.60; H, 10.56; N, 2.99. Found: C, 78.03; H, 10.36; N, 3.10.

Poly[2,5-didecyloxy-1,4-phenylene-*alt*-2,3-dimethyl-5,7-dithien-2-yl-thieno[3,4-*b*]pyrazine] (DP/DTTP, 3a). 281 mg of **DP** (0.4 mmol) and 194 mg of 2,3-dimethyl-5,7-dithien-2-yl-thieno[3,4-*b*]pyrazine] (0.4 mmol) were used to afford a black solid (yield: 50%). ^{1}H NMR (CD_2Cl_2, δ ppm): 7.61 (br, 2H), 7.41 (m, br, 4H), 4.07 (m, 4H), 2.67 (br, 6H), 1.97 (br, 4H), 1,26 (m, br, 28H), 0.84 (br, 6H). Anal. Calcd for $(C_{42}H_{54}N_2O_2S_3)_n$: C, 70.54; H, 7.61; N, 3.92; S, 13.45. Found: C, 70.92; H, 8.07; N, 3.44; S, 10.41.

Poly[2,5-didecyloxy-1,4-phenylene-*alt*-4,7-dithien-2-yl-2,1,3-benzothiadiazole] (DP/DTBT, 3b). 350 mg of **DP** (0.54 mmol) and 250 mg of 4,7-di-2-thienyl-2,1,3-benzothiadiazole (0.54 mmol) were used to afford a deep purple solid (yield: 60%). ^{1}H NMR ($CDCl_3$, δ ppm): 8.17 (br, 2H) 7.88(br, 2H), 7.69 (br, 2H), 7.37 (br, 2H), 4.11 (m, 4H), 2.03−1.25 (m, br, 32H), 0.87 (br, 6H) Anal. Calcd for $(C_{40}H_{50}N_2O_2S_3)_n$: C, 69.93; H, 7.34; N, 4.08; S, 14.00. Found: C, 68.02; H, 7.21; N, 3.85; S, 13.41.

Poly[2,5-didecyloxy-1,4-phenylene-*alt*-2,3-dimethyl-5,7-dithien-2-ylquinoxaline] (DP/DTQ, 3c). 350 mg of **DP** (0.54 mmol), 260 mg of 2,3-dimethyl-5,7-dithien-2-ylquinoxaline (0.54 mmol), and 15 mL of toluene were used to afford a light red solid (yield: 60%). ^{1}H NMR (CD_2Cl_2, δ ppm): 8.08 (br, 2H), 7.91 (br, 2H), 7.66 (br, 2H), 7.42 (br, 2H), 4.20 (br, 4H), 2.00 (br, 6H), 1.59 (br, 4H), 1.42−1.24 (br, 28H), 0.84 (br, 6H). Anal. Calcd for $(C_{44}H_{56}N_2O_2S_2)_n$: C, 74.53; H, 7.96; N, 3.95; S, 9.04. Found: C, 68.04; H, 6.87; N, 4.15; S, 10.00.

Characterization. ^{1}H nuclear magnetic resonance (NMR) data were recorded on a Bruker-AF300 spectrometer at 300 MHz. Gel permeation chromatographic (GPC) analysis was performed on a Laboratory Alliance RI2000 instrument (two column, MIXED-C and MIXED-D from Polymer Laboratories) connected with one refractive index detector from Schambeck SFD GmbH. All GPC analyses were manipulated on polymer/THF solution at a flow rate of 1 mL/min at 40 °C and calibrated polystyrene standards. Thermogravimetric analysis (TGA) and differential scanning calorimetry (DSC) measurements were performed under a nitrogen atmosphere at a heating rate of 20 and 10 °C/min using a TA Instruments TGA-951 and DSC-Q100, respectively.

UV−vis absorption spectra were recorded on a Perkin-Elmer model Lambda 900 UV/vis/near-IR spectrometer. The electrochemical properties of the polymer films were investigated on a Princeton Applied Research model 273A potentiostat/galvanostat with a 0.1 M acetonitrile or DMF solution containing tetrabutylammonium tetrafluoroborate ($TBABF_4$) as the electrolyte. Platinum wire and rod-tip electrodes were used as counter and working electrodes, respectively. Silver/silver ion (Ag in 0.1 M $AgNO_3$ in the supporting electrolyte solutions) was used as a reference electrode. A 3 wt % solution of a polymer in THF was used to prepare the polymer film on the Pt rod-tip electrode. Then, the cyclic voltammetry of films was performed on a three-electrode cell. The energy parameters HOMO and LUMO were estimated from the measured redox potentials on the basis of the prior work on conjugated polymers which has shown that HOMO $= -(E_{onset}^{ox} + 4.4)$ and LUMO $= -(E_{onset}^{red} + 4.4)$, where the onset potentials are in volts (vs SCE) and HOMO and LUMO are in electronvolts.[1d] The structures of polymer thin films on SiO_2/Si substrates were characterized by means of tapping mode atomic force microscopy (AFM) with a Nanoscope 3D controller (Digital Instruments). The cantilever used was fabricated from phosphorus-doped Si with a spring constant of 3 N/m and a resonance frequency of 82 kHz. The processing and annealing conditions of thin film of polymer samples are the same as the device fabrication to simulate the polymer transistor structures.

Fabrication and Characterization of Thin Film Transistors. Organic thin film transistors were prepared from polymer thin films with a bottom-contact configuration on the heavily n-doped silicon wafers. A thermally grown 200 nm SiO_2 used as the gate dielectric with a capacitance of 17 nF/cm^2. The aluminum was used to create a common bottom-gate electrode. The source/drain regions were defined by a 100 nm thick gold contact electrode through a regular shadow mask, and the channel length (L) and width (W) were 25 μm and 500 or 100 μm, respectively. Afterward, the substrate was modified with octyltrichlorosilane (OTS) as silane coupling agents. The 0.5 wt % polymer solutions in 1,2,4-trichlorobenzene should be filtered through 0.20 μm pore size PTFE membrane syringe filters, spin-coated at a speed rate of 1000 rpm for 60 s onto the silanized SiO_2/Si substrate, and heated at 60 °C overnight in vacuum. Output and transfer characteristics of the FET devices were measured using a Keithley 4200 semiconductor parametric analyzer. All the procedures and electrical measurements were performed in ambient air.

Fabrication and Characterization of Polymer Photovoltaic Cells. Before solar device fabrication, the ITO glass substrates were cleaned by ultrasonification sequentially in detergent, deionized water, acetone, and isopropyl alcohol. The synthesized polymers were dissolved in chloroform with the concentration of 10 mg/mL, followed by blending with PCBM and stirred overnight in the glovebox.

The polymer solar cell devices were fabricated by spin-coating a blend of polymer/PCBM, sandwiched between a transparent anode and a cathode. The anode consisted of glass substrates precoated with indium tin oxide (ITO), modified by spin-coating polyethylenedioxythiophene/polystyrenesulfonate (**PEDOT/PSS**) layer (∼30 nm), and the cathode consists of Ca (∼35 nm) capped with Al (∼130 nm). After device encapsulation, current−voltage characteristics of the devices under white-light illumination from AM 1.5 solar simulator (100 mW/cm^2) were recorded by a Keithley 2400 sourcemeter.

Table 1. Molecular Weight and Thermal Properties of the Donor−Acceptor Copolymers

polymer	M_w	M_n	PDI	T_d (°C)
DP/P	4350	3250	1.34	380
DP/TP	5440	4300	1.26	365
DP/BT	6120	4580	1.34	410
DP/Q	5100	3790	1.35	394
DP/Py	9500	5600	1.7	413
DP/DTTP	15 980	7640	2.09	381
DP/DTBT	9180	4560	2.01	400
DP/DTQ	3270	2820	1.16	393

Results and Discussion

Synthesis and Characterization. Figure 1 shows the representative ^{1}H NMR spectrum of the **DP/TP** copolymer (**2a**) in $CDCl_3$. The signals at 4.05 and 0.80−1.70 ppm are assigned to the protons on the *n*-decyloxy substituent chains. The peaks that appear at 7.95 and 7.47 ppm are due to the **TP** and phenylene protons, respectively. The numbers of aromatic and aliphatic protons estimated from peak integration are in a good agreement with the molecular structures of the copolymers. The ^{1}H NMR spectra of other polymers (Supporting Information) also showed a good agreement with the proposed polymer structures.

All the polymers except **2a** and **3c** were readily soluble in common solvents, such as chloroform, toluene, and chlorobenzene, whereas **2a** was completely soluble only at a high temperature. Polymer **3c** has a poor solubility in THF, chloroform, or toluene, but it shows good solubility in 1,2-dichlorobenzene at a high temperature. On the basis of the above polymer solubility results, chlorobenzene or dichlorobenzene was used as solvent for obtaining optical quality films for device characterization. The weight-average molecular weights (M_w) of the polymers was determined by gel permeation chromatography (GPC) against polystyrene standards in THF and found to be 3260−15 980 with a polydisperisty of 1.26−2.09, as shown in Table 1. The moderate molecular weight of the polymers probably results from the steric hindrance of the bulky didecyloxy group in the **DP** coupling monomer. The poor solubility of polymer **3c** in toluene probably inhibits the coupling reaction necessary for obtaining a high molecular weight polymer. The elemental analyses for carbon, hydrogen, nitrogen, and sulfur agree with the theoretical values, except polymers **3c**. The large deviation in the carbon content of polymer **3c** could be due to the bromine end groups since the GPC result also show it has a low molecular weight.

Figure 2 shows the thermogravimetric analysis (TGA) curves of the synthesized copolymers at the heating rate of 20 °C/min under a nitrogen atmosphere. As shown in the figure, the onset decomposition temperatures (T_d) of the copolymers are in the range of 365−413 °C, which suggests their good thermal stability. The small amount of weight loss before T_d in polymers **1** and **3c** probably attributed to the existence of low molecular weight oligomers. The differential scanning calorimetry (DSC) curves on all of the copolymers did not detect any clear phase transition and indicated that the movement of polymer chain was probably limited by the rigid-rod moiety.

Optical Properties. The normalized optical absorption of copolymers in dilute chloroform solution (10^{-5} M) and thin films are shown in Figures 3 and 4, respectively, and the corresponding absorption properties are collected in Table 2. The absorption maxima (λ_{max}) of polymers **DP/P** (**1**), **DP/TP** (**2a**), **DP/BT** (**2b**), **DP/Q** (**2c**), and **DP/Py** (**2d**) in solution are observed at 346, 605, 444, 379, and 383 nm, respectively, while those of thin films are at 352, 678, 457, 382, and 389 nm. The optical band gap (eV) obtained from the extrapolation of absorption edges of film are in the order of **2a** (1.47) < **2b** (2.37) < **2d** (2.76) < **2c** (2.78) < **1** (3.15). Note that the band gap of polymer **2d** is consistent with 2.84 eV of similar polymer structures with

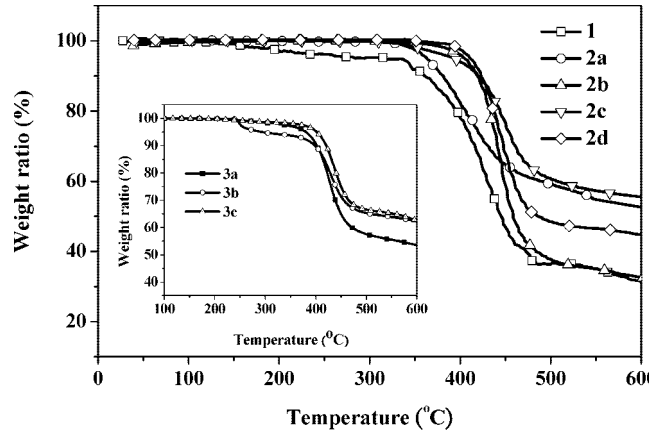

Figure 2. TGA curves of copolymers at the heating rate of 20 °C/min under a nitrogen atmosphere.

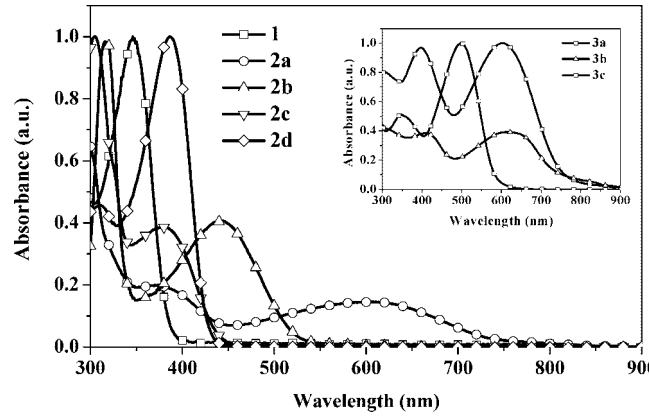

Figure 3. Optical absorption spectra of the copolymers in chloroform solutions.

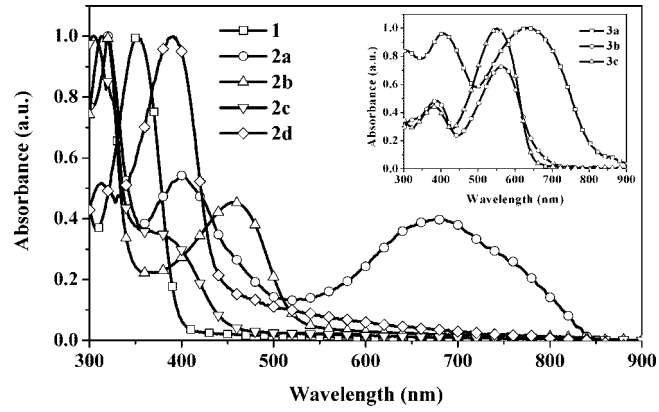

Figure 4. Optical absorption spectra of the copolymer films on glass substrates.

smaller alkoxyl substituent.[27] The lower band gaps of polymers **2a**−**2d** compared with that of parent polymer **1** are due to the intramolecular charge transfer (ICT) between the didecyloxyphenylene donor and **TP**, **BT**, **Q**, or **Py** acceptors. From the literature,[22] the order of the acceptor strength, **Q** < **TP** < **BT**, is not in agreement with a decreasing trend on the optical band gap of these alternative copolymers. Polymer **2a** shows two absorption bands (401 and 678 nm) attributed to the $\pi-\pi^*$ transition and ICT, respectively. The five-member ring backbone of the **TP** moiety leads to a smaller torsional angle than that of the **BT** moiety and promotes the efficient intramolecular charge transfer, which leads to the smaller band gap of the former. The optical band gap of polymer **2a** is the smallest among the

Table 2. Physical Properties of the the Donor−Acceptor Copolymers

polymers	$\lambda_{max}^{abs,sol}$ (nm)	$\lambda_{max}^{abs,film}$ (nm)	E_g^{opt} (eV)	E_{ox}^{onset} (V)	HOMO (eV)	E_{red}^{onset} (V)	LUMO (eV)	$E_g^{electro}$ (eV)	mobility (cm^2V^{-1} s^{-1})	on/off	rms[b] (nm)
DP/P	346	352	3.15	1.04	−5.44		−2.29[a]	3.15			
DP/TP	374, 605	401, 678	1.47	0.21	−4.61	−1.02	−3.38	1.23	1.89×10^{-3}	82	2.1
DP/BT	444	457	2.37	1.03	−5.43	−1.14	−3.26	2.17			
DP/Q	379	382	2.78	1.04	−5.44	−1.83	−2.57	2.87			
DP/Py	383	389	2.76	1.05	−5.45	−1.85	−2.55	2.90			
DP/DTTP	398, 602	410, 638	1.55	0.22	−4.62	−1.09	−3.31	1.31	1.41×10^{-5}	36	0.3
DP/DTBT	387, 564	413, 618	1.65	0.45	−4.85	−1.51	−2.89	1.96	1.92×10^{-4}	604	1.1
DP/DTQ	384, 497	381, 549	1.91	0.36	−4.76	−1.84	−2.56	2.20	2.10×10^{-3}	3600	0.7

[a] LUMO × band gap[opt] − HOMO. [b] Root-mean-square (rms) roughness from AFM measurement.

reported didecyloxyphenylene-based donor−acceptor conjugated polymers.

The λ_{max} of polymer films, **DP/DTTP** (**3a**), **DP/DTBT** (**3b**), and **DP/DTQ** (**3c**), are observed at 638, 618, and 549 nm, respectively, while the optical band gaps estimated from the absorption edges are 1.55, 1.65, and 1.91 eV, as shown in the inset of Figure 4. The incorporation of the two thiophene segments on the polymer backbone results in the significant red-shifted absorption on polymers **3b** and **3c** in comparison with polymers **2b** and **2c**. The large torsional angles of polymers **3b** and **3c** with six-member phenylene ring are probably reduced by incorporating the five-member thiophene ring,[2] which results in the more coplanar structures and enhanced π-electronic delocalization. However, polymer **3a** shows a slightly lager band gap than polymer **2a**. The planarity of the polymer backbone does not change significantly since the acceptor structures of **TP** and **DTTP** have a similar five-member ring. However, the acceptor/donor ratio decreases after incorporating the two thiophene rings, and it probably leads a reduced intramolecular charge transfer and enlarged band gap. Our recent study on the effect of copolymer ratio on the optical band gaps of thiophene/thieno[3,4-*b*]pyrazine copolymers also suggested a similar conclusion.[2d]

Electrochemical Properties. The electrochemical redox behaviors of synthesized copolymers with their cast thin films were characterized by cyclic voltammetry (CV). The oxidation and reduction cyclic voltammograms of polymer **1** and **2a**−**2d** are shown in parts a and b of Figure 5, respectively. The HOMO and LUMO levels of the polymers were estimated from the oxidation and reduction onsets, E_{ox}^{onset} and E_{red}^{onset}, respectively. The electrochemical band gap ($E_g^{electro}$) of the polymers were estimated from the difference between the E_{ox}^{onset} and E_{red}^{onset}. The electrochemical properties are summarized in Table 2. The estimated HOMO and LUMO energy levels of the parent polymer **1** are −5.44 and −2.29 eV, respectively. The HOMO energy level of polymers **2b**, **2c**, and **2d** are at −5.43 to −5.45 eV, which are very similar to that of polymer **1**. However, the LUMO levels of the polymers **2a**−**2d** are in the range of −2.55 to −3.38 eV, which is lower-lying than that of polymer **1**. The particular high-lying HOMO level (−4.61 eV) and low-lying LUMO level (−3.38 eV) of polymer **2a** are due to the coplanar polymer structures of the **TP** moiety. It also demonstrates the more efficient intramolecular charge transfer of polymer **2a** than the other three copolymers. Besides, polymer **2b** shows a lower-lying LUMO energy than polymers **2c** and **2d** since **BT** has the strongest π-electron accepting ability.[23] The electrochemical band gaps of polymers **2a**−**2d** are in the range of 1.23−2.90 eV, which are significantly lower than that of polymer **1** with 3.15 eV. The destabilization of HOMO and stabilization of LUMO level result in reduced band gaps, which also demonstrates the significance of intramolecular charge transfer through the donor−acceptor structures. Although there is deviation between the optical and electrochemical band gaps (0.2−0.8 eV), the trend between the band gap and polymer structure is similar. Polymer **3a** shows a similar HOMO level but a slighter higher LUMO level (Figure 5c) and electrochemical band gap than polymer **2a**, which could be explained by the less intramolecular charge transfer. Polymers **3b** and **3c** exhibit more higher-lying HOMO than **2b** and **2c**, respectively, indicating that the coplanarity of the polymer backbone is improved by incorporating the thiophene moiety.

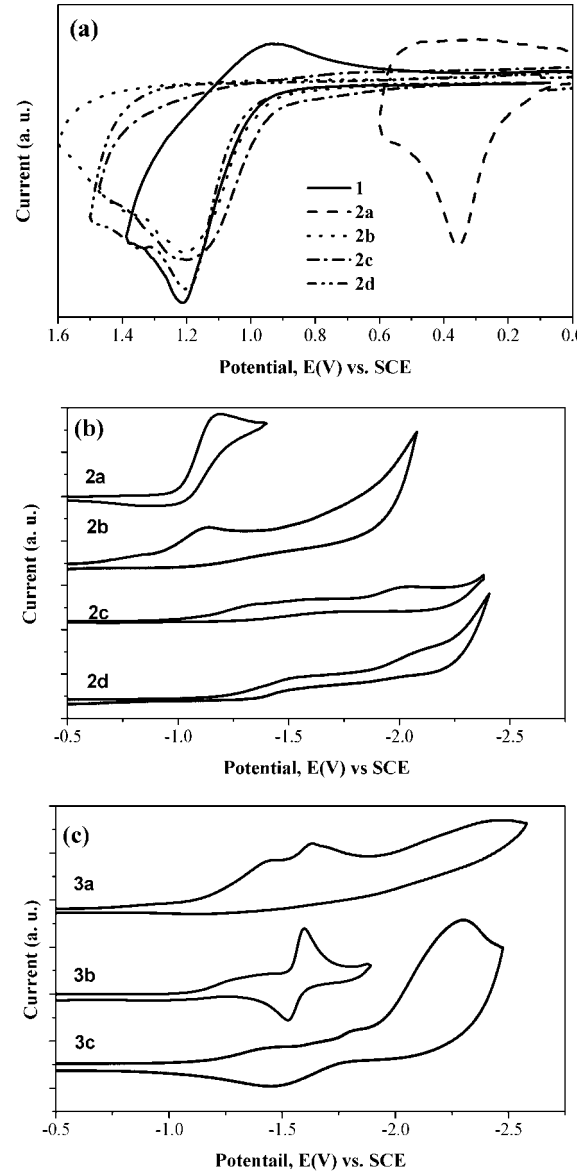

Figure 5. Cyclic voltammograms of copolymers thin film in 0.1 M $TBAPF_6$ solution: (a) electrochemical oxidation of polymers **1** and **2a**−**2d**; (b) electrochemical reduction of polymers **2a**−**2d**; (c) electrochemical reduction of polymers **3a**−**3c**.

Field-Effect Transistor Characteristics. The bottom contact FET devices based on the synthesized didecyloxyphenylene−

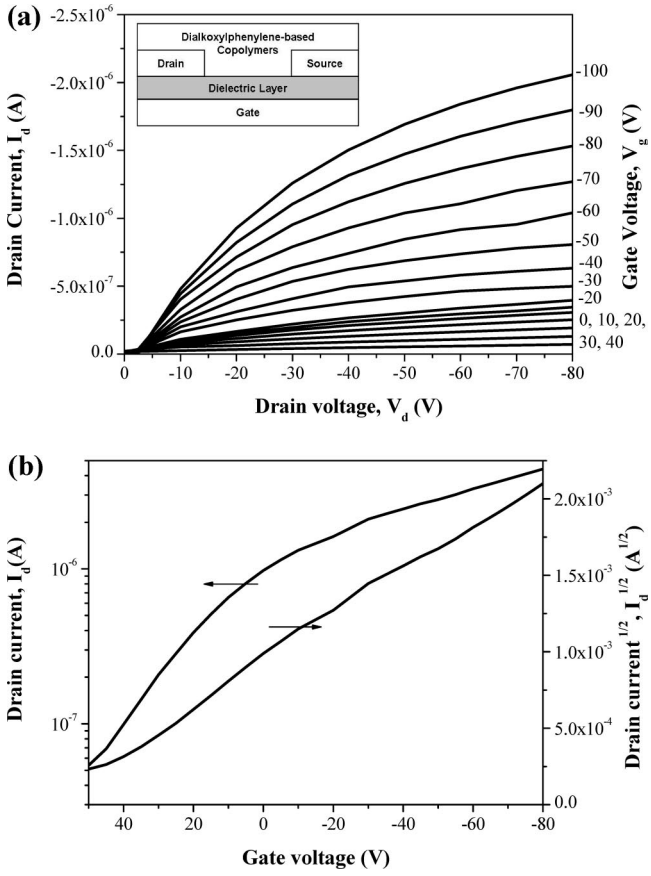

Figure 6. (a) Output and (b) transfer characteristics of polymer **2a** FET devices at $V_d = -80$ V in the saturation region for (b).

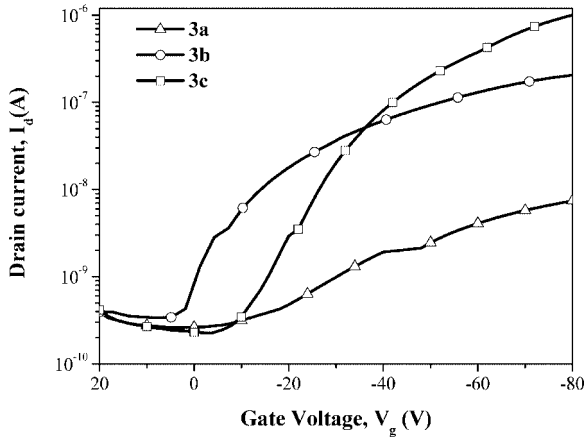

Figure 7. Transfer characteristics of polymers **3a**, **3b**, and **3c** FET devices at $V_d = -80$ V in the saturation region.

acceptor conjugated copolymers were fabricated on a Si/SiO_2 substrate by spin-coating. Only polymers **2a**, **3a**, **3b**, and **3c** device could show typical p-channel transfer characteristics (drain current (I_d) vs drain voltage (V_d) at various gate voltage (V_g)), as shown in Figures 6 and 7. In the saturation region ($V_d > V_g - V_t$), where V_t is the threshold voltage, I_d can be described by the equation

$$I_d = \frac{WC_i}{2L}\mu_{sat}(V_g - V_t)^2 \quad (1)$$

Here, W and L are the channel width and length, respectively. C_i is the capacitance of the gate insulator, μ_{sat} is the mobility in the saturation region, and V_t is the threshold voltage. Field-effect mobilities of the studied conjugated polymers were

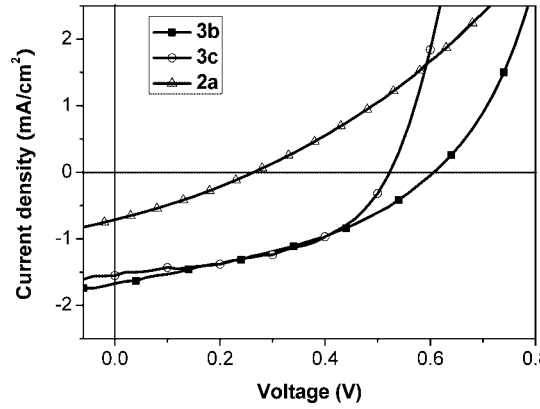

Figure 8. Current−voltage ($J-V$) characteristics of polymer **2a**/PCBM (1:1 w/w, open triangles) polymer **3b**/PCBM (1:3, w/w, filled squares), and polymer **3c**/PCBM (1:4 w/w, open circles) solar cells under simulated sunlight (AM1.5G, 100 mW/cm^2).

estimated by eq 1 and Figures 6 and 7. The estimated hole mobilities of polymers **2a**, **3a**, **3b**, and **3c** are 1.89×10^{-3}, 1.41×10^{-5}, 1.92×10^{-4}, and 2.1×10^{-3} cm^2 V^{-1} s^{-1}, respectively, with the corresponding on/off current ratios of 82, 36, 604, and 3.6×10^3 in ambient conditions. Although the obtained hole mobility is not as high as that of poly(3-hexylthiophene) (P3HT), it is comparable to the reported other classes of donor−acceptor conjugated polymers.[8,9] The high mobility (10^{-2}−10^{-1} cm^2 V^{-1} s^{-1}) of poly(3-hexylthiophene) is due to the regioregular polymer structure and resulted self-organized morphology. However, the synthesized DP−acceptor or DP−thiophene−acceptor−thiophene conjugated polymers do not have such regioregular polymer structure to obtain a similar mobility as P3HT. Also, the differential scanning calorimetry (DSC) curves on all of the copolymers did not detect any clear phase transition. The root-mean-square roughness (rms) of polymer films from the AFM are relatively low for the above four polymers, as shown in Table 2. It suggests the amorphorous characteristic of the synthesized polymers and the difference on the mobilities of the above polymers are most likely due to the polymer structures. Nevertheless, it would be of interest to discuss the effect of donor/acceptor strength and backbone planarity on the charge carrier mobility.

The significantly higher mobility of polymer **2a** than those of polymers **1** and **2b**−**2d** is probably due to the significant intermolecular charge transfer. Another possibility for the insignificant hole mobility of polymers **1** and **2b**−**2d** is that the high injection barrier based on the HOMO level (−5.54 to −5.45 eV). The obtained mobilities of polymers **2a** and **3c** are slighter larger than that of dialkoxylphenylene-*alt*-dodecylthiophene−TP−dodecylthiophene (**BTTP**−**P**) copolymer with 1.1×10^{-3} cm^2 V^{-1} s^{-1}.[9] The relatively low on/off current ratio of polymers **2a** and **3a** may be account for the high-lying HOMO energy levels of the polymers and thus the ambient oxygen doping of the organic semiconductor.[9] The low-lying HOMO level of polymer **3c** may be a main factor for the highest charge carrier mobility and large on/off current ratio of the polymer. It suggests that the low HOMO level of the polymer could provide enough stability for charge transporting and diminish the possibility of oxygen doping defects in ambient air.

Inserting thiophene segments into the six-member-ring backbones of polymers **2b** and **2c** not only manipulates optical and electrochemical properties but also enhances performances of field-effect transistors. Neither of polymers **2b** and **2c** exhibits any significant transistor characteristics, but high FET performances are observed from polymers **3b** and **3c** devices. It again demonstrates the importance of enhanced intramolecular charge

transfer by incorporating thiophene moieties. Nevertheless, the much lower charge transporting performance of polymer **3a** is observed, as compared with that of polymer **2a**. It is probably explained from the reduced intramolecular charge transfer[2c] or the change on the surface structure. By comparing the similar polymer reported by one of us,[9] the much higher mobility of **BTTP−P** than that of polymer **3a** is probably arisen from the self-assembly of alkyl chains in the former.[28,29] Moreover, the absence of the electron mobility of these synthesized materials is probably explained as below. The mismatch between the LUMO energy level of the studied copolymers and Au work function results in the significant energy barriers for electron injection, and thus electronic mobility was not observed.[7−9] The easily presence of electron trap center on the SiO_2 surface was an another important factor to mobile the electron difficultly.[7a]

Photovoltaic Cell Characteristics. The polymer photovoltaic cell was fabricated with a layered structure of glass/ITO/PEDOT:PSS/polymer−PCBM blend/Ca/Al. One of the key properties for polymer photovoltaic cell applications is the high carrier mobility (higher than or close to 10^{-3} cm^2 V^{-1} s^{-1} [4a,b]). The mobility of polymer **3a** is not high enough for obtaining significant power conversion efficiency, and thus only the photovoltaic cell characteristics of polymers **2a**, **3b**, and **3c** were studied. Figure 8 shows the current−voltage characteristics of the photovoltaic cells based on the three blends of polymer **2a**/PCBM (1:1 w/w), **3b**/PCBM (1:3 w/w), and **3c**/PCBM (1:4 w/w). Under white light illumination (100 mW/cm^2), the cell based on polymer **2a**/PCBM as the active layer has a short circuit current density (J_{sc}) of 0.71 mA/cm,^{2} an open circuit voltage (V_{oc}) of 0.27 V, a calculated fill factor (FF) of 0.33, and power conversion efficiency (PCE) of 0.06%. However, much enhanced device performance was found using the other two polymers: polymer **3b**/PCBM (1.67 mA/cm^2 (J_{sc}), 0.61 V (V_{oc}), 0.40 (FF), and 0.41% PCE; polymer **3c**/PCBM (1.55 mA/cm^2 (J_{sc}), 0.52 V (V_{oc}), 0.49 (FF), and 0.40% PCE.

V_{oc} is approximately a measure of the difference between the oxidation potential of the donor (polymers **2a**, **3b**, and**3c**) and the reduction potential of the acceptor (PCBM). Thus, the raising HOMO of polymer **2a**, closer to the LUMO of PCBM, diminishes the value of V_{oc} (0.27 V) while the V_{oc} of polymer **3b**/PCBM (0.61 V) and polymer **3c**/PCBM (0.52 V) shows a larger value. Furthermore, the J_{sc} of polymer **2a**/PCBM is lower than those of polymer **3b** or **3c**/PCBM. It might arise from the small energy difference (0.32 eV) between the LUMO levels of polymer **2a** (3.38 eV) and PCBM (3.7 eV) and lead to insufficient electron−hole charge separation. Therefore, polymer **2a**/PCBM shows a much lower power conversion efficiency than the others.

The highest power conversion efficiency for the polymers is around 0.41%, which is 1 order of magnitude smaller than that of poly(3-hexylthiophene) (P3HT)/PCBM-based devices.[5a,b] As described in the literature,[4a,b] small band gap, self-organized structure, and high carrier mobility are essential for obtaining high power conversion efficiency in bulk heterojunction solar cells. On the basis of the above criteria, the amorphorous characteristic of polymers **2** and **3** probably account for the observed low efficiency. However, their tunable electronic properties provide an understanding on how the polymer structures affect the device characteristics. Further optimization on the solar cell structure (such as different blend ratios, film thickness, or electrode materials) or processing conditions (such as annealing temperature) could lead to enhanced efficiency of photovoltaic cells.

Conclusions

In this study, seven soluble didecyloxyphenylene−acceptor or −thiophene−acceptor−thiophene copolymers were successfully synthesized by Suzuki coupling polymerization. The electronic, electrochemical, and optoelectronic properties significantly varied with acceptor strength and backbone planarity of the D−A copolymers. The copolymers showed a wide range of optical band gaps of 1.47−3.15 eV through the variation of acceptors. The field-effect mobility of holes varied from 1.4×10^{-5} cm^2 V^{-1} s^{-1} in **DP/DTTP** to 2.10×10^{-3} cm^2 V^{-1} s^{-1} in **DP/DTQ**. The observed much higher carrier mobilities in **DP/DTBT** and **DP/DTQ** copolymers than those of **DP/BT** and **DP/Q** are probably due to the improved backbone planarity of the latter. A power conversion efficiency around 0.4% was achieved from the photovoltaic cells fabricated from some of these polymers blended with PCBM. The present study demonstrates that the electronic and optical properties of dialkoxylphenylene-based donor−acceptor copolymers could be easily manipulated through the acceptor strength and backbone coplanarity.

Acknowledgment. The financial support from National Science Council and Ministry of Economics Affairs of Taiwan is highly appreciated. We thank Ms. M. H. Lai and Mr. C. F. Wang of National Taiwan University for technical assistance on polymer synthesis. Work at the University of Washington was supported by the Air Force Office of Scientific Research EHSS MURI (Grant FA9550-06-1-0326) and the NSF STC MDITR (DMR-0120967).

Supporting Information Available: ^{1}H NMR spectra of polymers **1**, **2b**, **2c**, **2d**, **3a**, **3b**, and **3c**. This material is free of charge via the Internet at http://pubs.acs.org.

References and Notes

(1) (a) Ego, C.; Marsitzky, D.; Becker, S.; Zhang, J.; Grimsdale, A. C.; Mullen, K.; MacKenzie, J. D.; Silva, C.; Friend, R. H. *J. Am. Chem. Soc.* **2003**, *125*, 437. (b) Tu, G. L.; Mei, C. Y.; Zhou, Q. G.; Cheng, Y. X.; Geng, Y. H.; Wang, L. X.; Ma, D. G.; Jing, X. B.; Wang, F. S. *Adv Funct. Mater.* **2006**, *16*, 101. (c) Liu, J.; Guo, X.; Bu, L. J.; Xie, Z. Y.; Cheng, Y. X.; Geng, Y. H.; Wang, L. X.; Jing, X. B.; Wang, F. S. *Adv. Funct. Mater.* **2007**, *17*, 1917. (d) Kulkarni, A. P.; Tonzola, C. J.; Babel, A.; Jenekhe, S. A. *Chem. Mater.* **2004**, *16*, 4556. (f) Kulkarni, A. P.; Kong, X. X.; Jenekhe, S. A. *Macromolecules* **2006**, *39*, 8699. (g) Zhu, Y.; Gibbons, K. M.; Kulkarni, A. P.; Jenekhe, S. A. *Macromolecules* **2007**, *40*, 804.

(2) (a) Wu, W. C.; Liu, C. L.; Chen, W. C. *Polymer* **2006**, *47*, 627. (b) Wu, W. C.; Chen, W. C. *J. Polym. Res.* **2006**, *13*, 441. (c) Lee, W. Y.; Cheng, K. F.; Wang, T. F.; Chueh, C. C.; Chen, W. C.; Tuan, C. S.; Lin, J. L. *Macromol. Chem. Phys.* **2007**, *208*, 1909. (d) Cheng, K. F.; Liu, C. L.; Chen, W. C. *J. Polym. Sci., Part A: Polym. Chem.* **2007**, *45*, 5872. (e) Wu, W. C.; Lee, W. Y.; Pai, C. L.; Chen, W. C.; Tuan, C. S.; Lin, J. L. *J. Polym. Sci., Polym. Phys.* **2007**, *45*, 67. (f) Tsai, F. C.; Chang, C. C.; Liu, C. L.; Chen, W. C.; Jenekhe, S. A. *Macromolecules* **2005**, *38*, 1958.

(3) (a) Xia, Y.; Deng, X.; Wang, L.; Li, X.; Zhu, X.; Cao, Y. *Macromol. Rapid Commun.* **2006**, *27*, 1260. (b) Peng, Q.; Peng, J. B.; Kang, E. T.; Neoh, K. G.; Cao, Y. *Macromolecules* **2005**, *38*, 7292. (c) Yang, R. Q.; Tian, R. Y.; Yan, J. G.; Zhang, Y.; Tang, J.; Hou, Q.; Yang, W.; Zhang, C.; Cao, Y. *Macromolecules* **2005**, *38*, 244.

(4) (a) Scharber, M. C.; Muhlbacher, D.; Koppe, M.; Denk, P.; Walfauf, C.; Heeger, A. J.; Brabec, C. J. *Adv. Mater.* **2007**, *18*, 794. (b) Coakley, K. M.; Mcgehee, M. D. *Chem. Mater.* **2004**, *16*, 4533. (c) Dennler, G.; Scharber, M. C.; Ameri, T.; Denk, P.; Forberich, K.; Waldauf, C.; Brabec, C. J. *Adv. Mater.* **2008**, *20*, 579. (d) Xin, H.; Kim, F. S.; Jenekhe, S. A. *J. Am. Chem. Soc.* **2008**, *130*, 5424. (f) Jenekhe, S. A.; Yi, S. *Appl. Phys. Lett.* **2000**, *77*, 2635.

(5) (a) Li, G.; Shrotriya, V.; Huang, J.; Yao, Y.; Moriarty, T.; Emery, K.; Yang, Y. *Nat. Mater.* **2005**, *4*, 864. (b) Kim, Y.; Cook, S.; Tuladhar, S. M.; Choulis, S. A.; Nelson, J.; Durrant, J. R.; Bradley, D. D. C.; Giles, M.; Mcculloch, I.; Ha, C. S.; Ree, M. *Nat. Mater.* **2006**, *5*, 197. (c) Peet, J.; Kim, J. Y.; Coates, N. E.; Ma, W. L.; Moses, D.; Heeger, A. J.; Bazan, G. C. *Nat. Mater.* **2007**, *6*, 497. (d) Wong, W. Y.; Wang, X. Z.; He, Z.; Djurisic, A. B.; Yip, C. T.; Cheung, K. Y.; Wang, H.; Mak, C. S. K.; Chan, W. K. *Nat. Mater.* **2007**, *6*, 521.

(6) (a) Campos, L. M.; Tontcheva, A.; Gunes, S.; Sonmez, G.; Neugebauer, H.; Sariciftci, N. S.; Wudl, F. *Chem. Mater.* **2005**, *17*, 4031. (b) Sivula, K.; Ball, Z. T.; Watanabe, N.; Frechet, J. M. J. *Adv. Mater.* **2006**, *18*, 209. (c) Zhang, F.; Mammo, W.; Andersson, L. M.; Admassie, S.;

Andersson, M. R.; Inganas, O. *Adv. Mater.* **2006**, *18*, 2169. (d) Tan, Z.; Hou, J.; He, Y.; Zhou, E.; Yang, C.; Li, Y. *Macromolecules* **2007**, *40*, 1868. (e) Hadipour, A.; de Boer, B.; Wildeman, J.; Kooistra, F. B.; Hummelen, J. C.; Turbiez, M. G. R.; Wienk, M. M.; Janssen, R. A. J.; Blom, P. W. M. *Adv. Funct. Mater.* **2006**, *16*, 1897. (f) Soci, C.; Hwang, I. W.; Moses, D.; Zhu, Z.; Waller, D.; Gaudiana, R.; Brabec, C. J.; Heeger, A. J. *Adv. Funct. Mater.* **2007**, *17*, 632. (g) Chang, Y. T.; Hsu, S. L.; Su, M. H.; Wei, K. H. *Adv. Funct. Mater.* **2007**, *17*, 3326.

(7) (a) Chua, L. L.; Zaumseil, J.; Chang, J. F.; Ou, E. C.; Ho, P. K. H.; Sirringhaus, H.; Friend, R. H. *Nature (London)* **2005**, *434*, 194. (b) Gadisa, A.; Perzon, E.; Andersson, M. R.; Inganas, O. *Appl. Phys. Lett.* **2007**, *90*, 113510. (c) Chen, M. X.; Crispin, X.; Perzon, E.; Andersson, M. R.; Pullerits, T.; Andersson, M.; Inganas, O.; Berggren, M. *Appl. Phys. Lett.* **2005**, *87*, 252105. (d) Babel, A.; Jenekhe, S. A. *J. Am. Chem. Soc.* **2003**, *125*, 13656.

(8) (a) Yamamoto, T.; Yasuda, T.; Sakai, Y.; Aramaki, S. *Macromol. Rapid Commun.* **2005**, *26*, 1214. (b) Yamamoto, T.; Kukubo, H.; Kobashi, M.; Sakai, Y. *Chem. Mater.* **2004**, *16*, 4616. (c) Champion, R. D.; Cheng, K. F.; Pai, C. L.; Chen, W. C.; Jenekhe, S. A. *Macromol. Rapid Commun.* **2005**, *26*, 1835. (d) Babel, A.; Zhu, Y.; Cheng, K. F.; Chen, W. C.; Jenekhe, S. A. *Adv. Funct. Mater.* **2007**, *17*, 2542.

(9) Zhu, Y.; Champion, R. D.; Jenekhe, S. A. *Macromolecules* **2006**, *39*, 8712.

(10) (a) Sonmez, G.; Shen, C. K. F.; Rubin, Y.; Wudl, F. *Angew. Chem., Int. Ed.* **2004**, *43*, 1498. (b) Sonmez, G.; Sonmez, H. B.; Shen, C. K. F.; Jost, R. W.; Rubin, Y.; Wudl, F. *Macromolecules* **2005**, *38*, 669. (c) Durmus, A.; Gunbas, G. E.; Toppare, L. *Chem. Mater.* **2007**, *19*, 6247.

(11) (a) Lin, Q. D.; Chang, F. C.; Song, Y.; Zhu, C. X.; Liaw, D. J.; Chan, D. S. H.; Kang, E. T.; Neoh, K. G. *J. Am. Chem. Soc.* **2006**, *128*, 8732. (b) Chu, C. W.; Ouyang, J.; Tseng, J. H.; Yang, Y. *Adv. Mater.* **2005**, *17*, 1440.

(12) Thompson, B. C.; Kim, Y. G.; McCarley, T. D.; Reynolds, J. R. *J. Am. Chem. Soc.* **2006**, *128*, 12714.

(13) Casado, J.; Ortiz, R. P.; Delgado, M. C. R.; Hernandez, V.; Raimundo, J. M.; Blanchard, P.; Allain, M.; Roncali, J. *J. Phys. Chem. B* **2005**, *109*, 16616.

(14) Thompson, B. C.; Kij, Y. G.; McCarley, T. D.; Reynolds, J. R. *J. Am. Chem. Soc.* **2006**, *128*, 1274.

(15) Yasuda, T.; Yamamoto, T. *Macromolecules* **2003**, *36*, 7513.

(16) Ono, K.; Adachi, A.; Okita, K.; Goto, M.; Yamashita, Y. *Chem. Lett.* **1998**, *6*, 545.

(17) Yasuda, T.; Imase, T.; Yamamoto, T. *Macromolecules* **2005**, *38*, 7378.

(18) Monkman, A. P.; Palsson, L.; Higgins, R. W. T.; Wang, C.; Bryce, M. R.; Batsanov, A. S.; Howard, J. A. K. *J. Am. Chem. Soc.* **2001**, *124*, 6049.

(19) Ng, S. C.; Lu, H. F.; Chan, H. S. O.; Fujii, A.; Laga, T.; Yoshino, K. *Adv. Mater.* **2000**, *12*, 1122.

(20) (a) Blouin, N.; Michaud, A.; Leclerc, M. *Adv. Mater.* **2007**, *19*, 2295. (b) Blouin, N.; Michaud, A.; Gendron, D.; Wakim, S.; Blair, E.; Neagu-Plesu, R.; Belletete, M.; Durocher, G.; Tao, Y.; Leclerc, M. *J. Am. Chem. Soc.* **2008**, *130*, 732. (c) Jenekhe, S. A.; Lu, L.; Alam, M. M. *Macromolecules* **2001**, *34*, 7315. (d) Lai, R. Y.; Kong, X.; Jenekhe, S. A.; Bard, A. J. *J. Am. Chem. Soc.* **2003**, *125*, 12631. (e) Knorr, A.; Daub, J. *Angew. Chem., Int. Ed. Engl.* **1995**, *34*, 2664.

(21) Grem, G.; Ledizky, G.; Ullrich, B.; Leising, G. *Adv. Mater.* **1992**, *4*, 36.

(22) Yang, Y.; Pei, Q.; Hegger, A. J. *J. Appl. Phys.* **1996**, *71*, 934.

(23) Kitamura, C.; Tanaka, S.; Yamashita, Y. *Chem. Mater.* **1996**, *8*, 570.

(24) Kenning, D. D.; Mitchell, K. A.; Calhoun, T. R.; Funfar, M. R.; Sattler, D. J.; Rasmussen, S. C. *J. Org. Chem.* **2002**, *67*, 9073.

(25) Pilgram, K.; Zupon, M.; Skiles, R. *J. Heterocycl. Chem.* **1970**, *7*, 629.

(26) Yamamoto, T.; Sugiyama, K.; Kushida, T.; Inoue, T.; Kanbara, T. *J. Am. Chem. Soc.* **1996**, *118*, 3930.

(27) Aubert, P. H.; Knipper, M.; Groenendaal, L.; Lutsen, L.; Manca, J.; Vanderzande, D. *Macromolecules* **2004**, *37*, 4087.

(28) Bao, Z.; Dodabalapur, A.; Lovinger, A. J. *Appl. Phys. Lett.* **1996**, *69*, 4108.

(29) Kline, R. J.; DeLongchamp, D. M.; Fischer, D. A.; Lin, E. K.; Richter, L. J.; Chabinyc, M. L.; Toney, M. F.; Heeney, M.; McCulloch, I. *Macromolecules* **2007**, *40*, 7920.

MA800488G